Supplementary Information for "Nodeless electron pairing in CsV_3Sb_5-derived kagome superconductors"

1. Summary of Fermi surface and identification of k_F

The Fermi Surface (FS) is obtained by integrating the angle-resolved photoemission spectroscopy (ARPES) intensity over ±5 meV around the Fermi level (E_F). Due to the limited detectable momentum area of the 5.8-eV laser source, we measured multiple samples to cover all the FS contours. We summarize the FS maps of the measured samples and the corresponding k_F points in Figs. S1 and S2 for $Cs(V_{0.86}Ta_{0.14})_3Sb_5$ (denoted hereafter as Ta0.14) and $Cs(V_{0.93}Nb_{0.07})_3Sb_5$ (denoted hereafter as Nb0.07), respectively.

The k_F is determined directly from the peak position of the integrated momentum distributed curve (MDC) at $T > T_c$ over E_F ± 2 meV. The peak position is obtained from a Lorentzian fit. It is worthy of note that although the β and δ FSs are close in momentum, the corresponding bands can be well distinguished. As shown in Figs. S1 and S2, the intensity of the β and δ bands are enhanced under different polarizations due to different V 3*d* orbital characters — *s*-polarization for the β FS and *p*-polarization for the δ FS.

2. Fitting procedure to obtain the amplitude of the SC gap

The SC gap amplitude was quantitatively determined by the fits based on the BCS spectral function[1,2], which has a form

$$A_{BCS}(k,\omega) = \frac{1}{\pi}\left[\frac{|u_k|^2\Gamma}{\left(\omega-\sqrt{\varepsilon_k^2+|\Delta(k)|^2}\right)^2+\Gamma^2}+\frac{|v_k|^2\Gamma}{\left(\omega+\sqrt{\varepsilon_k^2+|\Delta(k)|^2}\right)^2+\Gamma^2}\right]$$

where $|u_k|^2$ and $|v_k|^2$ are coherence factors for the occupied and unoccupied quasiparticles, respectively. Γ is the line width broadening factor due to the finite quasiparticle lifetime. $E_k=\sqrt{\varepsilon_k^2+|\Delta(k)|^2}$ is the Bogoliubov quasiparticle band dispersiosn, ε_k is the band dispersion near E_F in the normal state, $|\Delta(k)|$ is the SC gap amplitude. In order to fit the ARPES data, the BCS spectral function is multiplied by the Fermi-Dirac function and convoluted with a Gaussian function corresponding to the experimental energy resolution. Then the EDCs at k_F, obtained by integrating the ARPES intensity over k_F ± 0.02 Å^{-1}, are fitted to extract the SC gap $|\Delta(k)|$.

3. Statistics of the fitted SC gap amplitude measured on different samples

By applying the fitting procedure to the EDCs at k_F on the different FSs, we obtain the momentum dependence of the SC gap amplitude, which directly reflects the pairing symmetry. As presented in Figs. 2g and 3g in the main text, we observed the SC gap amplitudes of the Ta0.14 and Nb0.07 samples are both nearly isotropic in the momentum space. To demonstrate the small fluctuation of the SC gap amplitudes, we present the statistics of the fitted SC gap amplitudes for the Ta0.14 samples in Table S1, and for the Nb0.07 samples in Table S2. The average deviations are less than 0.04 meV, which means a very small fluctuataction around the average value of SC gap amplitude ($\overline{\Delta}$). Moreover, the difference between the maximum and minimum values of the SC gap amplitudes, Δ_{max} - Δ_{min}, is comparable to the two times of the standard deviation of E_F (~0.06 meV), which determines the error bars for the SC gap. These demonstrate that the SC gap amplitude is almost constant in different momenta, supporting a nearly isotropic pairing gap symmetry. The consistent SC gap observed in different samples demonstrates the high quality of the single crystals and excludes the sample-dependent influences on the SC gap.

4. Superconducting gap at difference k_z

The FS maps of the Nb0.07 sample at k_z = 4.5π/c and 4.8 π/c are plotted in Figs. S4a and S4d, which are measured with 5.8-eV and 7-eV laser, respectively. Here we apply an inner potential of 7.3 eV[3] to convert photon energies to k_z, as shown in the inset of Fig. S4g. The EDCs at k_F on the β FS are shown in Fig. S4b for 5.8-eV laser and Fig. S4e for 7-eV laser. The corresponding symmetrized EDCs are shown in Figs. S4c and S4f, respectively.

Because the energy resolution for the measurements with 7-eV laser is about twice larger than that with 5.8-eV, the coherence peak of the EDCs measured at k_z = 4.8 π/c is broader than that measured at k_z = 4.5 π/c. To effectively compare the SC gap at these two different k_z, the EDCs are fitted with the function described in Note 2, with the energy resolution taken into account. The extracted SC gap amplitudes at these two k_z planes are summarized in Fig. S4g, which clearly shows that they are nearly the same within experimental uncertainties.

5. Spectral evidence of the electron-phonon coupling

The electron-phonon coupling (EPC) is ubiquitous in quantum materials, which could induce the kinks in the band dispersion at the frequencies of the coupled phonons. As shown in Figs. S6a-c, the kinks are observed on the α and β bands for all the pristine, Nb0.07 and Ta0.14 samples. These kinks are more prominent in the extracted band dispersions from the fits of the MDCs, as shown in Figs. S6d-f. For the α band, the kink is at the binding energy E_B of ~30 meV, while for the β band two kinks are distinguished at E_B of ~10 meV and 30 meV.

Generally, the superconductivity could be promoted if there is a stronger EPC. Indeed, the EPC is enhanced for the Nb0.07 and Ta0.14 samples which have a higher T_c compared to the pristine sample. The EPC strength can be estimated by the ratio between the Fermi velocity and the velocity of the bare band. Here the bare band is the band dispersion without the effect of EPC, which is assumed as a line between a high E_B and E_F. As shown in Fig. S6g, with the V partially substituted by the Nb/Ta, the EPC strength on the β band (derived from V 3*d* orbitals) is prominently enhanced, while the EPC strength on the α band (derived from Sb 5*p* orbital) remains nearly a constant. Such enhancements of EPC in the samples with higher T_c further support an EPC driven superconductivity.

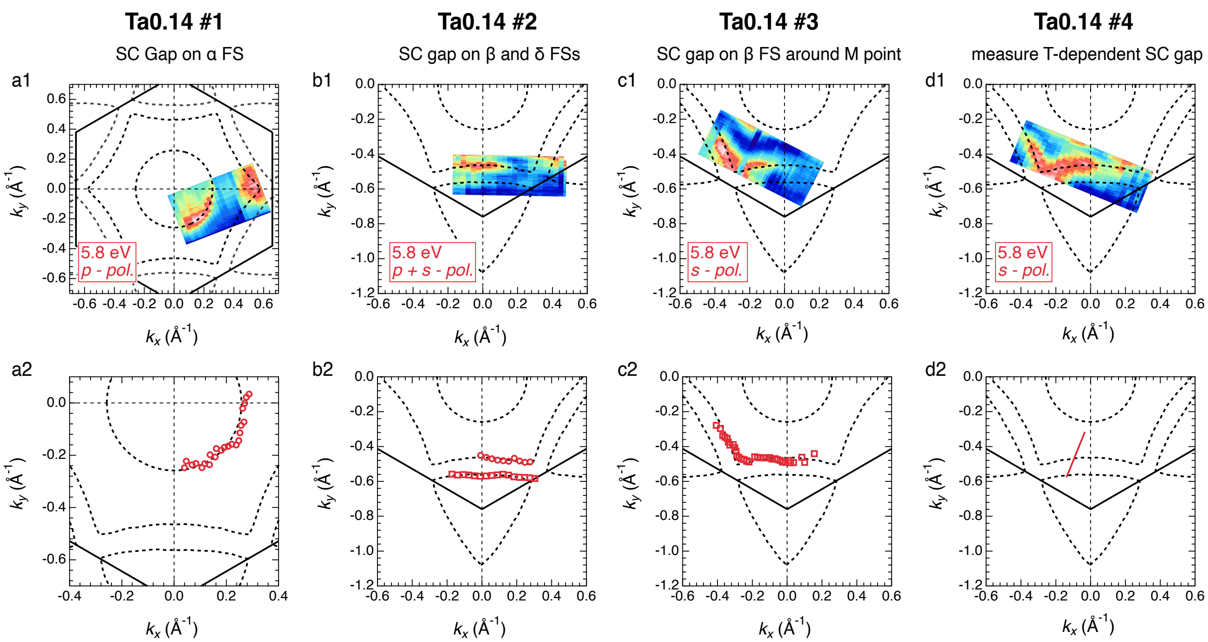

Fig. S1. Fermi surface of all measured Ta0.14 samples and the k_F points at which superconducting gap is measured.

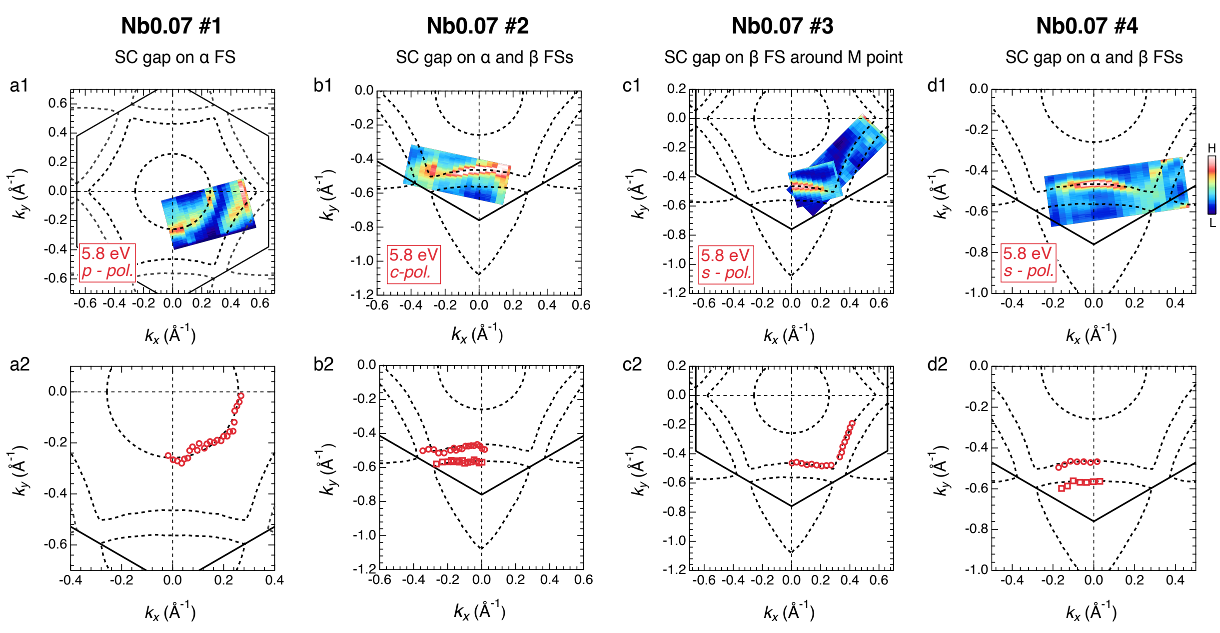

Fig. S2. Fermi surface of all measured Nb0.07 samples and the k_F points at which superconducting gap is measured.

Samples	**k_F along with**	**k_F numbers**	**$\bar{\Delta}$ (meV)**	**Average deviation**	**Δ_{max}- Δ_{min}**	**$2\bar{\Delta}/k_BT_c$**
Ta0.14 #1	α FS	23	0.78	0.03	0.16	3.48
Ta0.14 #2	β FS	10	0.76	0.02	0.08	3.40
	δ FS	16	0.77	0.04	0.16	3.44
Ta0.14 #3	β FS (around M)	34	0.78	0.03	0.21	3.48
Average			0.77	-	-	3.44

Table S1. Statistics of the SC gap for the Ta0.14 samples with T_c ~ 5.2 K. The SC gap amplitudes on different FSs of different samples are highly consistent and averaged at 0.77 meV, giving $2\Delta/k_BT_c$ of 3.44.

Samples	**k_F along with**	**k_F numbers**	**$\bar{\Delta}$ (meV)**	**Average deviation**	**Δ_{max}- Δ_{min}**	**$2\bar{\Delta}/k_BT_c$**
Nb0.07 #1	α FS	25	0.55	0.03	0.17	2.87
Nb0.07 #2	β FS	18	0.48	0.03	0.16	2.52
	δ FS	15	0.51	0.02	0.08	2.67
Nb0.07 #3	β FS (around M)	17	0.52	0.02	0.10	2.75
Nb0.07 #4	β FS	7	0.59	0.02	0.10	3.12
	δ FS	7	0.58	0.03	0.11	3.04
Average			0.54	-	-	2.83

Table S2. Statistics of the SC gap for the Nb0.07 samples with T_c ~ 4.4 K. The SC gap amplitudes on different FSs of different samples are comparable and averaged at 0.54 meV, giving a ratio $2\Delta/k_BT_c$ of 2.83.

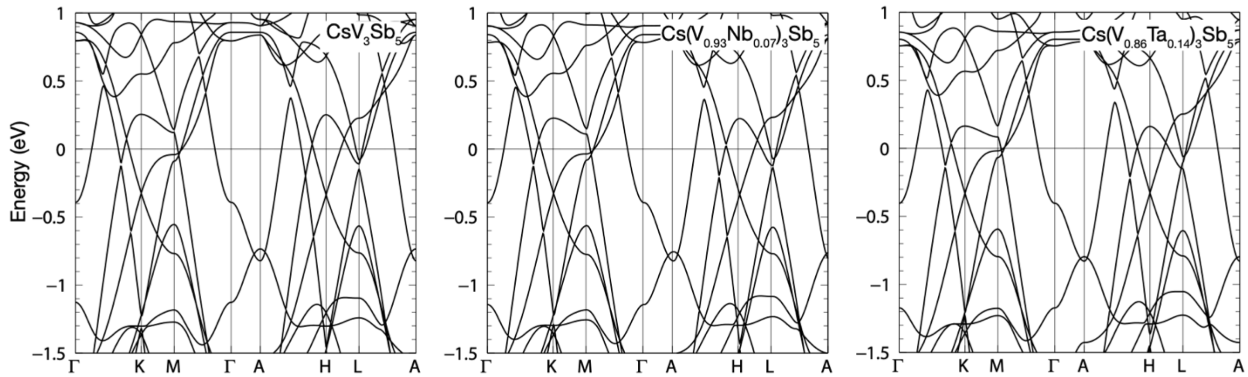

Fig. S3. Caculated band structures for the CsV_3Sb_5, $Cs(V_{0.93}Nb_{0.07})_3Sb_5$ and $Cs(V_{0.86}Ta_{0.14})_3Sb_5$ samples based on density functional theory. The experimentally determined lattice constants are used in the calculation. The overall band structure is not dramatically changed upon Nb/Ta substitutions of V.

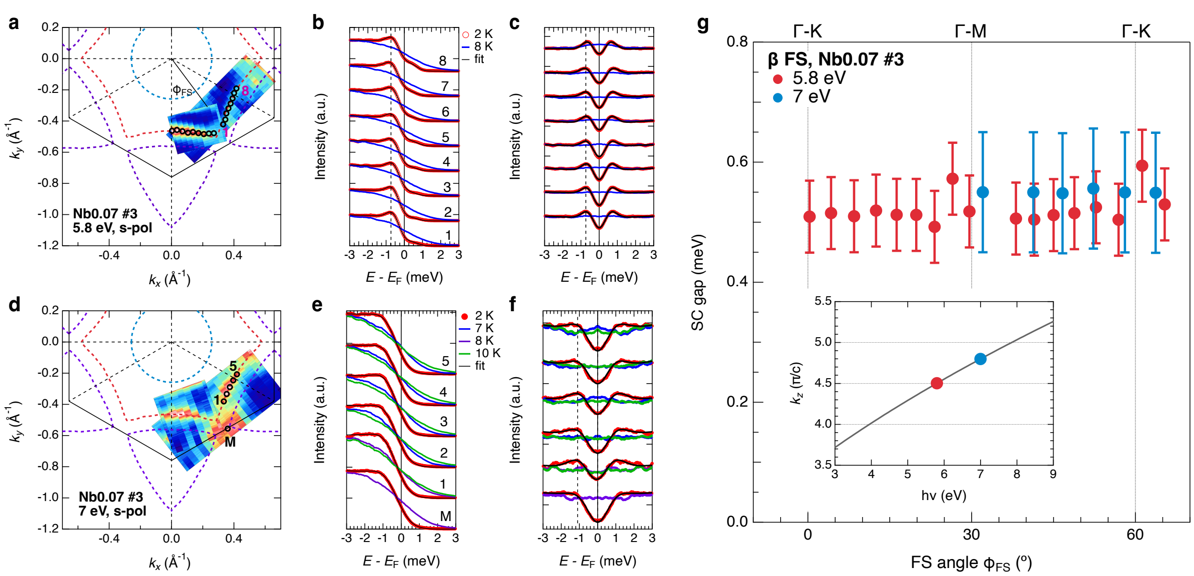

Fig. S4. Superconducting gap at different k_z for the Nb0.07 sample. a, FS map taken with 5.8-eV laser. **b,** EDCs at k_F marked in **a**. The black lines are the fits of these EDCs. **c**, Symmetrized EDCs for **b**. **d-f**, Same as **a-c** but for the data taken with 7-eV laser. The curves are vertically offset for clarity. **g**. Comparison of the SC gap amplitude measured with 5.8-eV and 7-eV laser. The inset shows the k_z positions corresponding to these two photon energies.

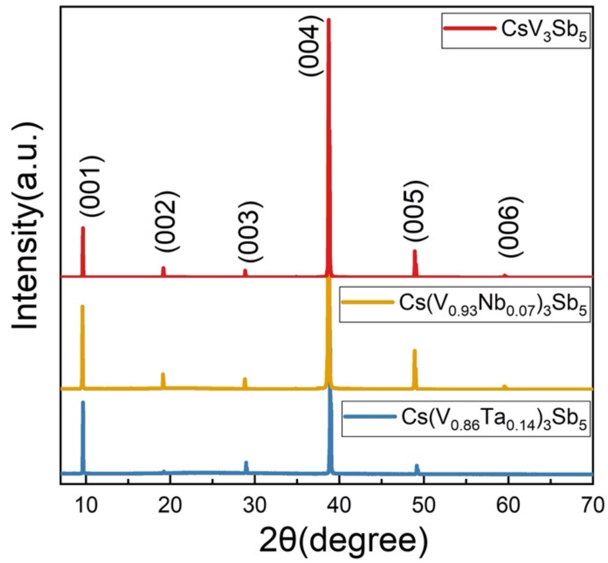

Fig. S5. X-ray diffraction pattern of the pristine CsV_3Sb_5, Nb0.07 and Ta0.14 single crystals.

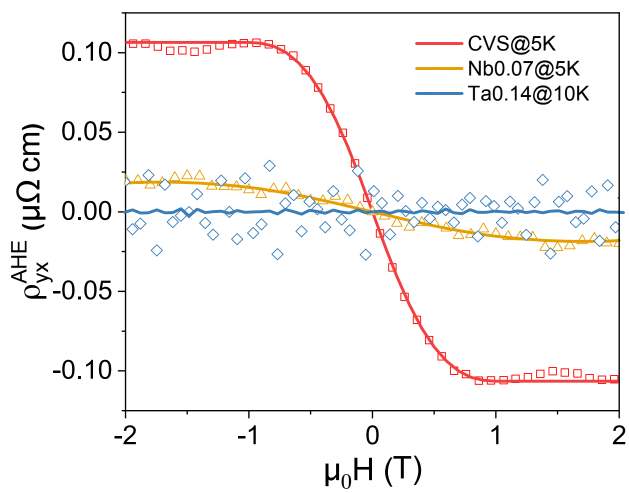

Fig. S6. Comparison of the anomalous Hall resistance ρ_{yx}^{AHE} in pristine CsV_3Sb_5, Nb0.07 and Ta0.14 samples, which is weakened in the Nb0.07 sample and absent in the Ta0.14 sample. ρ_{yx}^{AHE} is extracted by subtracting the local linear ordinary Hall background.

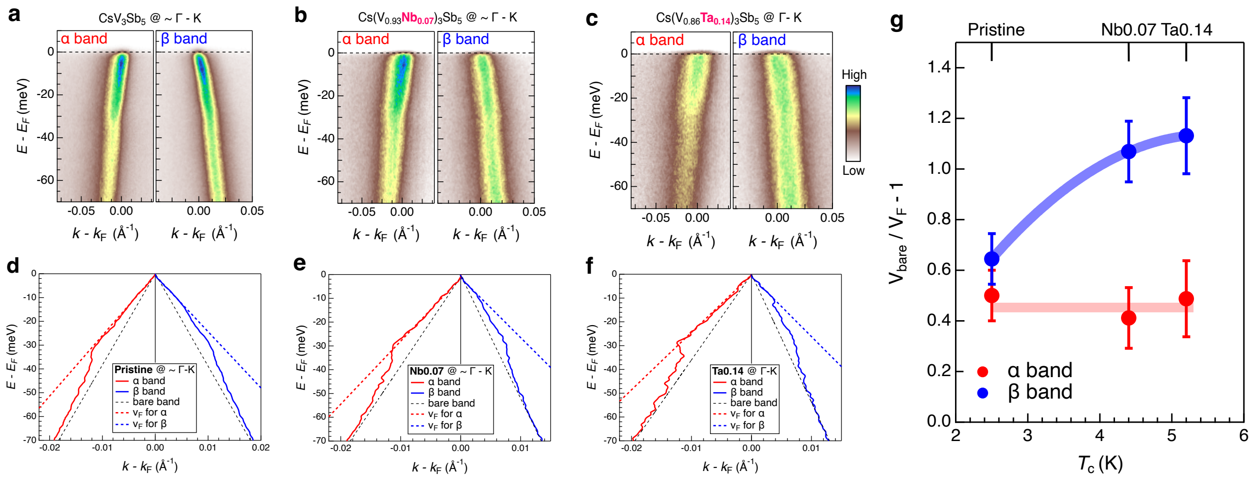

Fig. S7. Spectral evidence of the electron-phonon coupling. a-c, ARPES intensity plots of the α and β bands nearly along Γ–K direction for the pristine CsV_3Sb_5, Nb0.07 and Ta0.14 samples, respectively. These ARPES data are taken with 7-eV laser at $T = 6$ K. **d-f**, Extracted band dispersions. **a** and **d** are adopted from the Reference[4], in which the T_c of the measured CsV_3Sb_5 is ~ 2.5 K. **g**, Ratio between the velocity of the bare band and the Fermi velocity for the pristine, Nb0.07 and Ta0.14 samples, plotted as a function of their T_c.

References:

1 Matsui, H. *et al.* BCS-like Bogoliubov quasiparticles in high-T_c superconductors observed by angle-resolved photoemission spectroscopy. *Physical Review Letters* **90**, 217002 (2003).

2 Shimojima, T. *et al.* Orbital-independent superconducting gaps in iron pnictides. *Science* **332**, 564-567 (2011).

3 Li, C. *et al.* Spectroscopic Evidence for a Three-Dimensional Charge Density Wave in Kagome Superconductor CsV_3Sb_5. *arXiv:2112.06565* (2021).

4 Zhong, Y. *et al.* Testing electron-phonon coupling for the superconductivity in Kagome metal CsV_3Sb_5. *arXiv:2207.02407* (2022).